Optimization of Polyethylene Grade Transitions in Fluidized Bed Reactors with Constraints on the Polymer Sticking Temperature

Sabrine Kardous, Timothy Mckenna, Nida Sheibat-Othman

Optimization of polyethylene grade transitions in fluidized bed reactors with constraints on the polymer sticking temperature

Sabrine Kardous[1], Timothy F.L. McKenna[2], Nida Sheibat-Othman[1*]

[1] Université of Lyon, Université Claude Bernard Lyon 1, CNRS, UMR 5007, LAGEPP, F-69622, Villeurbanne, France

[2] Université of Lyon, Université Claude Bernard Lyon 1, CPE Lyon, CNRS, UMR 5265, C2P2, Villeurbanne, France.

[*]E-mail : nida.othman@univ-lyon1.fr

Abstract

In gas-phase polyolefin processes, it is important to evaluate the melting temperature of particles since exceeding this temperature may cause particle sticking and aggregation. In this work, a model combining thermodynamic aspects and representing the evolution of the physical properties of the polymer is used to predict the melting onset temperature of polyethylene particles in a fluidized bed reactor. In this way, the model accounts for the effects of the polymer density and particle swelling by penetrants on the melting temperature. This model is then used within an optimization strategy to control the transition between different polymer grades, while avoiding particle sticking. The controlled properties are the polymer density and melt index, and the manipulated variables are the flow rates of hydrogen and comonomer and the bed temperature. Constraints are considered on the upper and lower limits of the flow rates. The bed temperature was constrained to remain lower than the polymer onset melting temperature, with a safety margin. It is shown that controlling the properties while respecting the constraints is feasible over a specific range.

Keywords

Fluidized bed reactor; Polymer melting temperature; Grade transition; Off line dynamic optimization; Thermodynamic model.

Introduction

Fluidized bed reactors (FBRs) are the most efficient reactors for the commercial-scale production of polyethylene in the gas-phase in terms of heat evacuation. To better enhance the heat removal capacity of FBRs and allow higher reaction rates, many polyolefin processes operate under condensed mode cooling.[1] However, the addition of induced condensing agents (ICA) that aid in temperature control, as well as comonomers, affects the degree of swelling of the polymer which in turn can influence polymer properties and reaction rates.[2] It has thus been pointed out by several groups that adapted thermodynamic models are required to allow precise prediction of the reaction rate and polymer properties in presence of such additives.[3,4] Not only is it important to understand the impact of these additives at steady state operation, but it is also essential to understand their impact during grade transitions when significant changes in the flow rates of different species are required. In a recent work,[5] the importance of employing an adapted thermodynamic model during grade transition was demonstrated in the case of the copolymerization of ethylene with 1-hexene or 1-butene in presence of ICA (n-hexane or isobutane). An offline dynamic optimization methodology was developed to control the polymer density and melt index by manipulating the flow rates of hydrogen and comonomer. Other works treated the optimization of grade transition, but the thermodynamic effects were not accounted for.[6,7,8]

Another issue in gas phase reactions is related to particle sticking that may occur if the reaction temperature is close enough to the melting temperature of the polymer particles. If a fraction of the polymer in the growing particles begins to melt this can cause the outer layers to become

stickier and stickier, eventually leading to particle aggregation, which can influence the quality of fluidization, as well as to fouling or blocking of the distributor plate.[9,10] It is therefore essential to maintain control of the reactor temperature at all times. Generally speaking, one wishes to keep it low enough that the particle does not stick, but high enough that the productivity of the system is not compromised.[11–15]

The melting temperature of particles is linked to the amount of comonomer incorporated in the polyethylene (PE) chain. The rate of incorporation of comonomer depends on the amount of comonomer absorbed in the amorphous polymer (to be calculated by an adapted thermodynamic model) as well as the type of catalyst and its ability to incorporate comonomer.[16,17] A second polymer property that may affect the particle melting temperature is the polymer molecular weight. Significant fractions of low molecular weight polymer, including the low molecular weight tail of a broad molecular weight distribution were found to promote particle sticking.[18] The type of catalyst also plays an important role, as besides its impact on the incorporation of comonomer and the average molecular weight, it may influence the distribution of branches and the molecular weight distribution. Finally, the swelling of a polymer by different penetrants will also have a strong influence on the melting temperature of polyethylene. ICAs such as n-pentane or n-hexane or α-olefin comonomers, all of which are commonly found in a gas phase process, can impact the effective melting temperature of the polymer in the reactor.[19,20]

In this work, we consider the optimization of transition between different polymer grades (defined by the polymer density and melt index) in a fluidized bed reactor of polyethylene. Attention was paid during the optimization to keep the reactor temperature lower than the polymer sticking point (and thus avoid particle sticking and ensure good particle fluidization and process safety). A model based on data collected from the patent literature will be used to define a stickiness limit of the dry polymer. Then, using Flory-Huggins theory, the effect of

swelling on the particle melting temperature is calculated. A classic kinetic copolymerization model is used and the bed is considered to behave as a CSTR. Super dry conditions are assumed, where the comonomer and ICA are injected under gaseous form. Three systems are considered: copolymerization of ethylene with 1-butene and copolymerization of ethylene with 1-hexene in the presence or absence of the ICA n-hexane. A thermodynamic model based on Sanchez-Lacombe equation of state (SL EoS) is used for both ternary systems and an approximation is made for the quaternary system based on a previous work.[5] Based on these results, simplified thermodynamic models are then proposed to allow for fast computation within the optimization loop.

In the following section, the main parts of the model are presented, including the prediction of the sticking temperature, the thermodynamic model, the kinetics, and the mass and energy balances. In section three the optimization and control methodologies are presented. Finally, simulations are realized and the results discussed.

Modelling the reactor and polymer properties

2.1 Defining the sticking temperature

It is difficult to know how to calculate precisely when the polymer becomes too sticky, as this depends on a number of factors linked to a number of polymer properties, the temperature of the polymer particles and to the reactor operating conditions. Experimental methods have been proposed to measure the melting temperatures of polymer as a function of the polymer density, molecular weight and comonomer type.[21] Also, the effect of the particle swelling by ICA on the melting temperature was evaluated. Hari et al. related the melt initiation temperature (MIT) of polyethylene particles evaluated by differential scanning calorimetry to the sticking temperature experiments done in a stirred autoclave.[22] They developed an empirical linear

correlation of the sticking temperature as a function of an effective isopentane mass fraction in the gas phase. The decrease in the sticking temperature could reach 10°C when doubling the fraction of isopentane in some situations. As a result, the more the polymer was amorphous (so less dense, but also able to swell with more ICA or comonomer), the faster the stickiness limit was reached.[23] This notion of using the melt onset, or melt initiation temperature as an indication of the temperature at which a polymer will begin to melt and to stick has been discussed in several patents, and will be considered in this work.

The concept can be shown in Figure 1 where 2 hypothetical melting thermograms are pictured, one for a dry polymer and one for a polymer swollen by one or more penetrants. When the dry polymer is heated, the polymer chains start losing their rigidity, become deformable then start to melt.[16] The MIT can be defined as the point where the tangent to the baseline and the tangent going through the inflection point in the rising part of the melt curve intersect, while the temperature at the peak of the curve is usually identified as the melting temperature (T_m). Swelling the polymer by one or more penetrants causes a depression in T_m, and will also reduce the MIT. The melt point depression (ΔT_m) and the reduction in the *MIT* (ΔMIT) can be defined as follows:

$$\Delta T_\mathrm{m} = T_{\mathrm{m},0} - T_\mathrm{m}$$
$$\Delta MIT = MIT_0 - MIT \quad (1)$$

Where $T_{\mathrm{m},0}$ and T_m refer to the melting temperatures of the unswollen (dry) and swollen polymer respectively. Similarly, MIT_0 and MIT refer to the melt initiation temperatures of the dry and swollen polymer respectively.

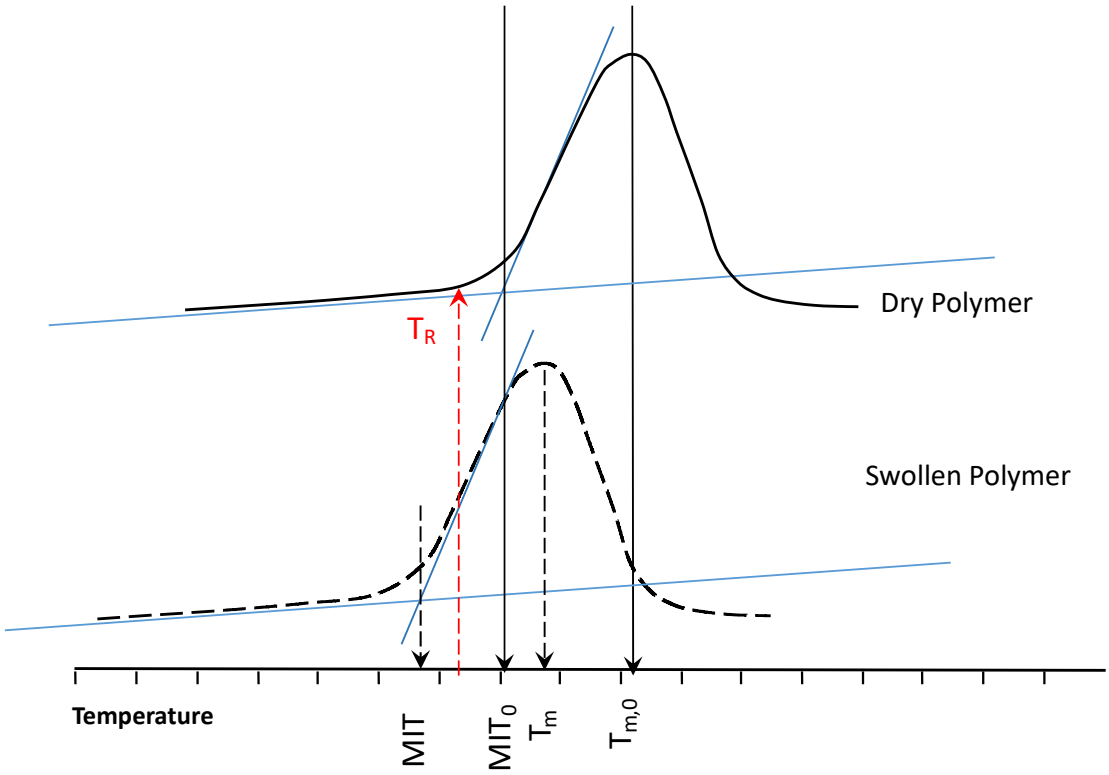

Figure 1. Scheme of the definition of the melt initiation temperature (MIT), and the changes incurred in the values of the MIT and melting temperature of a dry polymer when it is swollen with a mixture of penetrants.

The *MIT* appears to be the closest to the sticking temperature and will thus be adopted in this work.[22] Note that other works related the sticking to the softening of particles such the well-known Vicat softening temperature or the method suggested by Chmelar et al.[16]. However, while the softening temperature is most likely correlated with stickiness as it determines when the polymer becomes deformable, the initiation of melting represents a better indication of when the polymer becomes dangerously sticky.

In general, one tries to operate the FBR at a temperature few degrees lower than the *MIT*. This means that if the FBR is operated at a temperature T_R under dry conditions as shown in Figure 1, then it should be possible to avoid a lot of sticking of the polymer. However, if one were to change the feed composition to bring the reactor to the swollen conditions shown in this same figure without changing the reactor temperature, then the reactor would be operating at a point higher than the *MIT* and we would run the risk of significant sticking of the polymer. Ideally

one would like to be able to predict the impact of swelling directly on the *MIT*. In the following sections, we first discuss the estimation of the melting temperature of a dry polymer (here called T_{m0}), in the absence of swelling, then we investigate the influence of swelling on the swollen particle melting temperature (here called T_{m}).

T_{m0} and MIT_0 of dry polymer

In the case of linear low density polyethylene (LLDPE), the melting temperature of a dry polymer first depends on the type and amount of α-olefin comonomers incorporated into the LLDPE chain.[24] The most commonly used α-olefin comonomers for producing LLDPE are 1-butene and 1-hexene. The melting temperature for several commercial grades of LLDPE is correlated with the polymer density in Figure 2.[21] The data shown here are for a mixture of 1-butene and 1-hexene-based copolymers, produced using Ziegler-Natta and mixed metallocene catalysts. It is well-known that both the comonomer type and catalyst type will have an impact on the melting behavior of the product. Zeigler-Natta catalysts have broader molecular weight distributions than do single site catalysts and also favor the incorporation of more comonomer in the low molecular weight chains, whereas metallocenes have a uniform comonomer incorporation. This will of course lead to different MIT for similar densities, so the data in Figure 2 should not be used indiscriminately for all LLDPE processes and products. For the scope of the current paper, suffice to say that the better one is able to correlate the MIT with process variables (comonomer type, catalyst type, number of reactors in series, etc.), the more robustly one can push the limits of the grade change policy. In the current paper, we choose to use this correlation to demonstrate the importance of considering this type of information, and how to account for it in developing a grade change policy. Also, the values of the melt flow index (*MI*) at 2.16 kg are $0.45 < MI < 20$, suggesting that for this range of values the molecular weight does not have a significant influence on the melting temperature. Similarly, Hari et al.[22]

provided data on the *MIT* as a function of LLDPE density. Once again, a linear correlation between the *MIT* and polymer density appears to provide a good estimate of the value of this important temperature. We will use the correlation shown in this figure to calculate the dry *MIT* of the LLDPE as a function of its density. The influence of the *MI* or molecular weight on the *MIT* was not indicated, so we will suppose that the polymer molecular weight does not have a significant impact on the *MIT*, as observed on the same figure for $T_{m,0}$. The effect of the molecular weight on $T_{m,0}$ was found in the literature to become negligible above 10 kg mole^{-1}.[25]

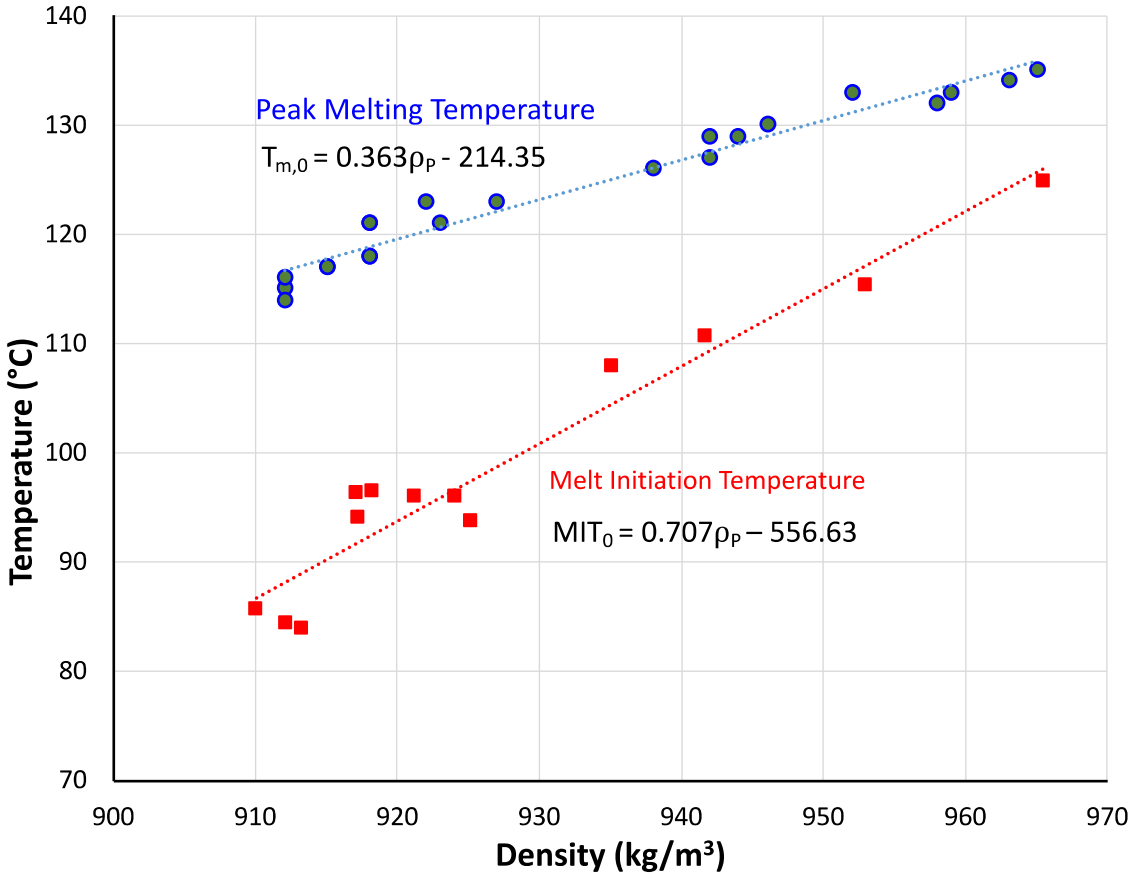

Figure 2. Peak melt temperatures ($T_{m,0}$) for a range of commercial LLDPE and HDPE powders[21], and the MIT_0, also for a range of different commercial polymers[22]. Both temperatures are shown as a function of the polymer density.

Note that also fundamental models were proposed to predict the melting temperature, $T_{m,0}$, of polyethylene as a function of the polymer density, polymer molecular weight and comonomer type, such as the model of Kamal et al. based on Flory theory.[25] However, models such as this last one rely on a number of simplifying assumptions to describe what is a complex phenomenon, and often do not fit well to experimental data for which they were not developed. We therefore chose to rely on the empirical data-based correlations presented above. Moreover, as indicated above, we prefer using the predictions of MIT_0, which is supposed to be more representative of the sticking temperature than $T_{m,0}$.

T_m of swollen polymer

It is worth noting that the gases that dissolve in the amorphous phase of the polymer do not necessarily act as sticking promoters per se. The penetrants which are known to act as sticking promoters are ICAs and comonomers. Low molecular weight species, or those with low solubility in the amorphous phase, such as ethylene and hydrogen, do not act as sticking promoters.[18]

A model of the polymer melting temperature that accounts for the presence of sorbed species that swell the particle was suggested by Flory-Huggins theory:[26]

$$\frac{1}{T_\mathrm{m}} - \frac{1}{T_{\mathrm{m},0}} = \frac{R}{\Delta H_\mathrm{u}} \frac{V_\mathrm{u}}{V_\mathrm{d}} \left(\phi_\mathrm{d} - \chi \phi_\mathrm{d}^2\right) \qquad (2)$$

Where T_m is the equilibrium melting temperature of the polymer-penetrant mixture and $T_{\mathrm{m},0}$ is the melting temperature of dry polymer (here obtained by the correlation in Figure 2). The same equation will be applied for *MIT* instead of T_m. V_u is the volume of the repeat unit (38 Å^3 for ethylene molecule, the comonomer impact being neglected here). V_d is the volume of the penetrants assumed to act as sticking promoters (73 Å^3 for 1-butene molecule, 107.6 Å^3 for 1-hexene[27], can also be ICAs) and ϕ_d is the volume fraction of these penetrants. χ is the

temperature- and concentration-dependent Flory-Huggins interaction parameter for which different measurement methods and models have been proposed.[28,29,30] It describes the miscibility of the penetrant into the polymer: χ >0.55 indicates that the penetrant is immiscible, 0.3<χ<0.55 indicates a moderate miscibility and χ<0.3 indicates a good miscibility.[31] Note that the melting point depression in Flory-Huggins theory characterizes the decrease of the melting point of a polymer due to the mixing with another species (penetrant) and occurs only if the two species (PE and penetrant) are miscible or partially miscible.[32]

Simulations of the Flory-Huggins equation combined with the correlation of MIT_0 presented in the previous section are shown in Figure 3. The penetrant 1-butene is considered. It can be seen that the effect of density is very important as it may reduce MIT_0 from 100°C to 90°C when decreasing the density from ρ_p=930 to 915 kg m^{-3}, in the absence of penetrant . Swelling by the penetrant by ϕ_d=10 % may decrease MIT_0 by 6°C. Finally, the figure shows that in the region of coherent fractions of penetrant in the polymer (i.e. ϕ_d<20%), the interaction parameter χ has a negligible influence on MIT. Therefore, χ can be fixed at 0.5 and there is no need for using a detailed model to compute it for the present application.

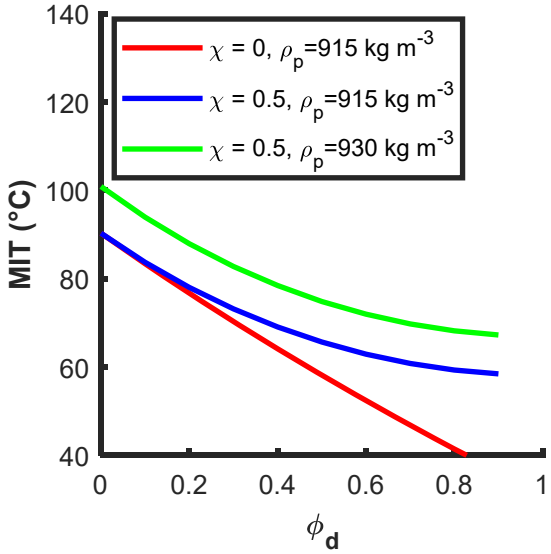

Figure 3. Effects of the polymer density, ρ_p, and volume fraction of penetrant , ϕ_d, on the melting initiation temperature of the swollen or dry polymer.

This model will be used to calculate the melting point depression due to swelling, and we make the approximation that $\Delta T_{\mathrm{m}} \approx \Delta MIT$, therefore $MIT = MIT_0 - \Delta MIT$. There is no guarantee that $\Delta T_{\mathrm{m}} \approx \Delta MIT$, as these values will depend on a number of physical characteristics of the polymer. However, in the absence of concrete data it seems to be a reasonable assumption to equate the two. The reactor temperature for the swollen polymer must be less than or equal to this new value of *MIT*. Generally, one can add a "safety margin" to this *MIT* value, as a function of the catalyst and the type of the polymer, between 1-10°C.[33] In the current work, we will choose a value of 5°C.

2.2 Thermodynamic model

The objective of the thermodynamic model is to calculate the concentrations of monomer and comonomer in the polymer particles which are required to calculate the reaction rates. Moreover, it allows to calculate the volume fraction of the penetrant ϕ_{d} required in the Flory-Huggins equation to compute the melting temperature of swollen polymer. The thermodynamic model used to calculate these concentrations is the Sanchez-Lacombe equation of state (SL EoS), but one may use other methods like the PC-SAFT EoS. This model uses interaction parameters, k_{ij}, that are temperature-dependent, that need to be identified at the operating temperature and pressure ranges. Their identification is discussed in the following subsections for each of the studied systems. Three systems are considered: copolymerization of ethylene with 1-butene and copolymerization of ethylene with 1-hexene in presence or absence of the ICA n-hexane. Based on the SL EoS results, a simplified thermodynamic model is developed to allow faster computation within the optimization loop (see next subsection).

In the process model, it is also required to evaluate the polymer crystallinity, x_{i}. The crystallinity is known to vary with the comonomer content in the polymer chains.[34] Chmelar et

al.[16] indicated that the polymer crystallinity varied linearly with the polymer density. Based on their work, the following relation was identified:

$$x_{\mathrm{i}} = x_{\mathrm{i},1}\,\rho_{\mathrm{p}} - x_{\mathrm{i},2} \tag{3}$$

The parameters $x_{\mathrm{i},1}$ and $x_{\mathrm{i},2}$ are given in Table 1.

Simplified thermodynamic model

In order to allow the implementation of the thermodynamic model within the optimization loop, the obtained results from the SL EOS are approximated by polynomials of degrees 1 or 2, as suggested by Alves et al.[35] (Table 1). For the used systems, the concentrations of ethylene in the polymer particles, $\left[M_1^{\mathrm{p}}\right]$, and of comonomer (1-butene or 1-hexene), $\left[M_2^{\mathrm{p}}\right]$, as a function of the particle crystallinity, x_{i}, and the operating conditions (pressure *P,* and temperature *T*), are given by:

$$\left[M_1^{\mathrm{p}}\right] = \left[M_1^{\mathrm{p,am}}\right](1 - x_{\mathrm{i}}) = [AP_2 + B](1 - x_{\mathrm{i}}) \tag{4}$$

$$\left[M_2^{\mathrm{p}}\right] = \left[\mathrm{M}_2^{\mathrm{p,am}}\right](1 - x_{\mathrm{i}}) = \left[C{P_2}^2 + DP_2\right](1 - x_{\mathrm{i}}) \tag{5}$$

where *A*, *B*, *C* and *D* are temperature-dependent parameters (Table 1) and $\left[M_i^{\mathrm{p,am}}\right]$ is the concentration of monomer *i* in the amorphous polymer.

Another result of the SL EoS is the volume fraction of the penetrant ϕ_{d} required in the Flory-Huggins equation to calculate T_{m}. A polynomial correlation can also be developed to allow for fast calculation of ϕ_{d} during the optimization, as follows:

$$\phi_{\mathrm{d}} = EP_2^2 + FP_2 \tag{6}$$

where *E* and *F* are temperature-dependent model parameters (Table 1). Note that P_2 is replaced by $P_2 + P_{\mathrm{ICA}}$ in the quaternary system involving comonomer and ICA.

As FBRs may operate at different temperatures, it is required to extend the model parameters to be variable over the operating range of temperature. Based on SL EoS, these parameters can be identified for different temperatures and a linear relation could be identified (Table 1).

The hydrogen concentration in the polymer can be calculated from the solubility $S_{\mathrm{H_2}}$ (g H_2 per g of amorphous polymer), using Henry's law:[36]

$$\left[H_2^{\mathrm{p}}\right] = \left[H_2^{\mathrm{p,am}}\right](1 - x_{\mathrm{i}}) = S_{\mathrm{H_2}} \frac{\rho_{\mathrm{p,am}}}{M_{\mathrm{w,H_2}}}(1 - x_{\mathrm{i}}) \qquad (7)$$

with $S_{\mathrm{H_2}} = 10^{-5} k_{\mathrm{H_2}} P_{\mathrm{H_2}}$, and the solubility coefficient is $\log_{10} k_{\mathrm{H_2}} = -1.323 - 304.8 \left(\frac{T_{\mathrm{c,H_2}}}{T}\right)$. $\rho_{\mathrm{p,am}}$ is the amorphous polymer density, $M_{w,\mathrm{H_2}}$ the hydrogen molecular weight, $T_{\mathrm{c,H_2}}$ its critical temperature and $P_{\mathrm{H_2}}$ its pressure (Pa). It is assumed that hydrogen exhibits no non-ideal thermodynamic interactions (so no cosolubility effect) with the other species in the reactor.

Table 1. Coefficients of the correlations of the ternary systems ethylene/1-butene/LLDPE and ethylene/1-hexene/LLDPE (P (bar), T(K), $\left[M_i^{p,am}\right]$ (mole m^{-3}))

		1-butene	1-hexene	Units
Relation \ Validity domain		P_1=7 bar P_2=[1.55-10] bar T=[70-90] °C	P_1=10 bar P_2=[0-1] bar T=[80-90] °C	
$\left[M_1^{\mathrm{p,am}}\right] = [AP_2 + B]$ $A = A_1 T + A_2$ $B = B_1 T + B_2$	A_1	-0.019	-2.24	mol m^{-3} bar^{-2} K^{-1}
	A_2	8.29	819	mol m^{-3} bar^{-2}
	B_1	0.018	-1.75	mol m^{-3} bar^{-1} K^{-1}
	B_2	125.8	906	mol m^{-3} bar^{-1}
$\left[M_2^{\mathrm{p,am}}\right] = \left[C{P_2}^2 + DP_2\right]$ $C = C_1 T + C_2$ $D = D_1 T + D_2$	C_1	0	-16.85	mol m^{-3} K^{-1}
	C_2	0	6162	mol m^{-3}
	D_1	-1.35	-30.2	mol m^{-3} bar^{-2} K^{-1}
	D_2	612.44	11539	mol m^{-3} bar^{-2}
$\phi_{\mathrm{d}} = EP_2^2 + FP_2$ $E = E_1 T + E_2$ $F = F_1 T + F_2$	E_1	0	-0.001	bar^{-2} K^{-1}
	E_2	0	0.37	bar^{-2}
	F_1	-0.0001	-0.0038	bar^{-1} K^{-1}
	F_2	0.053	1.44	bar^{-1}
$x_{\mathrm{i}} = x_{\mathrm{i,1}}\, \rho_{\mathrm{p}} - x_{\mathrm{i,2}}$	x_{i1}	0.007		m^3 kg^{-1}
	x_{i2}	-5.84		-

k_{ij} of the system ethylene/1-butene/LLDPE

In this ternary system, ethylene is used as monomer (component 1), 1-butene as commoner (2) and LLDPE (3) is the used polymer. Note that the interaction parameters between small molecules can be assumed to be ideal, so k_{12}=0.[4] The other parameters, i.e. the interaction parameter of ethylene with polymer, k_{13}, and 1-butene with polymer, k_{23}, need to be identified based on ternary data, as it is not possible to use binary data due to the cosolubility (i.e. the presence of 1-butene increases the solubility of ethylene compared to a binary system) and antisolvent effects (i.e the presence of ethylene reduces the solubility of 1-butene). Ternary data of this system is available at 70°C within a total pressure of monomer plus comonomer in the range of 2.5-4 bar, for which the interaction parameters k_{ij} were identified (Table 2).[37] It is required to extrapolate these parameters to 90°C and to a wider range of pressure. For this extension, few assumptions were made, but the estimations can be improved once ternary data becomes available at 90°C and under the real operating pressure. First of all, a slight exponential decrease of k_{ij} with the temperature was observed in some works, but a linear correlation can lead to a satisfactory approximation.[38,39] Binary data of 1-butene in LLDPE-1-butene are available at different temperatures 30-88°C and pressures 0-15 bar.[40] From this binary data, the slope of variation of the k_{ij} parameters with temperature can be determined and employed in the ternary system.[5] Using the identified k_{ij} parameters within SL EoS, the solubility can be estimated at 70°C and 90°C and over a wider monomer and comonomer pressure ranges (P_1=7 bar, P_2=1.55-10 bar). A linear relation of these concentrations can then be identified at different temperatures. The obtained parameters are predicted as a function of temperature as explained in the previous section (Table 1).

Figure 4 shows the results of the SL EoS as well as the linear correlations predicting the concentrations of ethylene and 1-butene in the amorphous polymer. A slight cosolubility effect of 1-butene on ethylene can be observed, while a big anti-solvent effect of ethylene on 1-butene

appears when comparing to binary data in LLDPE-1-butene. Figure S1 (Supporting Information) shows the variation of the volume fraction of the comonomer as calculated by SL EoS from which a linear correlation could be identified.

Table 2. Binary interaction parameters of the ternary system ethylene/1-butene/LLDPE, P_1=7 bar, P_2=0-10 bar (k_{12}=0 ethylene/1-butene).

Temperature	Ethylene/LLDPE k_{13}	1-butene/LLDPE k_{23}
70°C [37]	-0.09495	0.04618
90°C	-0.1089	0.0302
***T*=[70-90]°C**	$k_{13} = -6.98 \times 10^{-4}\, T(K) + 0.144$	$k_{23} = -7.99 \times 10^{-4}\, T(K) + 0.32$

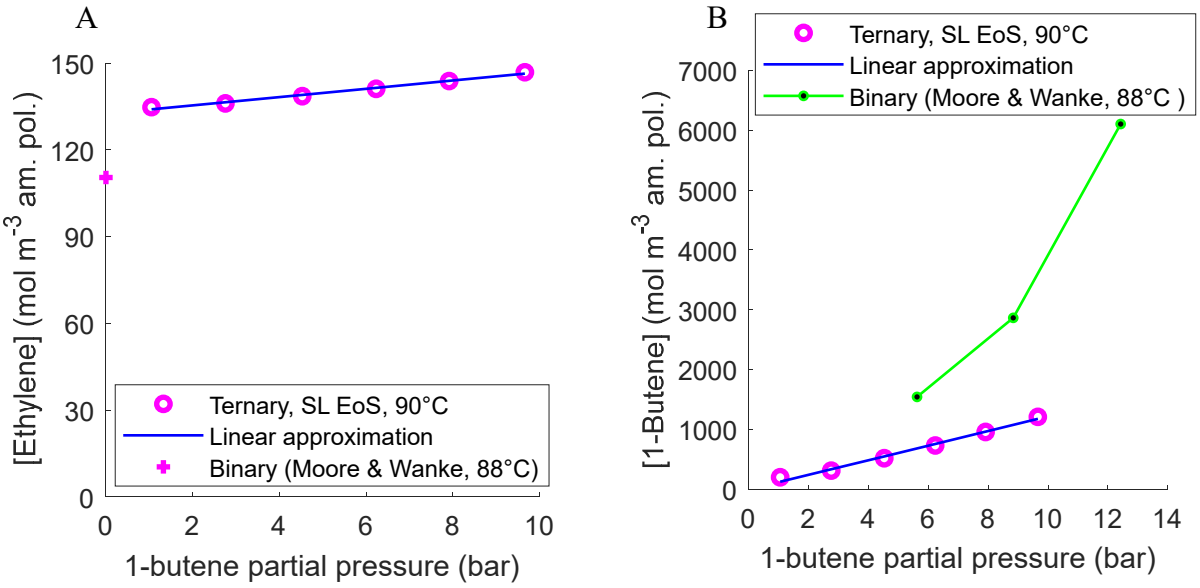

Figure 4. Estimated concentrations in LLDPE amorphous phase using SL EoS for the ternary system ethylene/1-butene/LLDPE, at 90°C and 7 bar of ethylene: A) ethylene and B) 1-butene. Comparison with binary data.[40]

k_{ij} of the system ethylene/1-hexene/LLDPE

The ternary system here consists of the monomer ethylene, comonomer 1-hexene and polymer LLDPE. As there are no available thermodynamic data for this system, it is assumed that 1-

hexene behaves like n-hexane for which ternary solubility data is available (Yao et al.[41]), as suggested by Alizadeh et al.[4] This approximation is reasonable as 1-hexene and n-hexane have similar binary solubility data in PE and they are comparable in structure. Therefore, the available ternary solubility data for the system ethylene/n-hexane/LLDPE[41] is used to estimate the k_{ij} for the current system (see Table 3).[4] The identified parameters are valid for a comonomer pressure range of 0-1 bar and 10 bar ethylene. It is to be noted that 1-hexene has a much higher solubility in the polymer than 1-butene.[40] As for the first system, a simplified thermodynamic model was derived to estimate $[M_1^{\mathrm{p}}]$, $[M_2^{\mathrm{p}}]$ and ϕ_{d} as a function of temperature. For the quaternary system ethylene/1-hexene/n-hexane/LLDPE, the k_{ij} where approximated in a previous work by considering a pseudo species englobing 1-hexene and n-hexane, based on the fact that they have the same solublity in a binary system.[5]

Table 3. Binary interaction parameters of the ternary system ethylene/1-hexene/LLDPE, P_1=10 bar, P_2=0-1 bar (k_{12}=0 Ethylene/1-hexene).

Temperature	Ethylene/LLDPE k_{13} [4]	1-hexene/LLDPE k_{23}
80°C	-0.022	0.0145
90°C	-0.032	0.021
***T*=[80-90]°C**	$k_{13} = -0.001\,T(K) + 0.331$	$k_{23} = 6.5 \times 10^{-4}\,T(K) - 0.215$

2.3 Mass and energy balances

All commercial scale FBR are continuous reactors and operate in a bubbling fluidization regime (Figure 5). The vapor phase rises through the bed from the bottom to the top, where it is evacuated, compressed, cooled and recycled. The superficial gas velocity inside the bed is usually 3-6 times higher than the fluidization velocity (50-70 cm s^{-1}) and the single-pass monomer conversion is about 2-5 %. The polymer powder is said to generally rise up through the center of the bed where the velocity is higher, and then fall back down the reactor walls in a roughly toroidal flow pattern, with an internal recirculation time on the order of minutes. The

powder phase is also continuously withdrawn and sent for degassing, then pelletized. This high solid recirculation rate with respect to the product withdrawal rate (consequently a reactor residence times on the order of few hours), combined with a per pass conversion of the gas phase on the order of 5-10 %, allows one to approximate the residence time distribution of an FBR with that of an ideal.[6,42,43] Note that although the per pass conversion is low, the overall conversion tends to be above 95%.

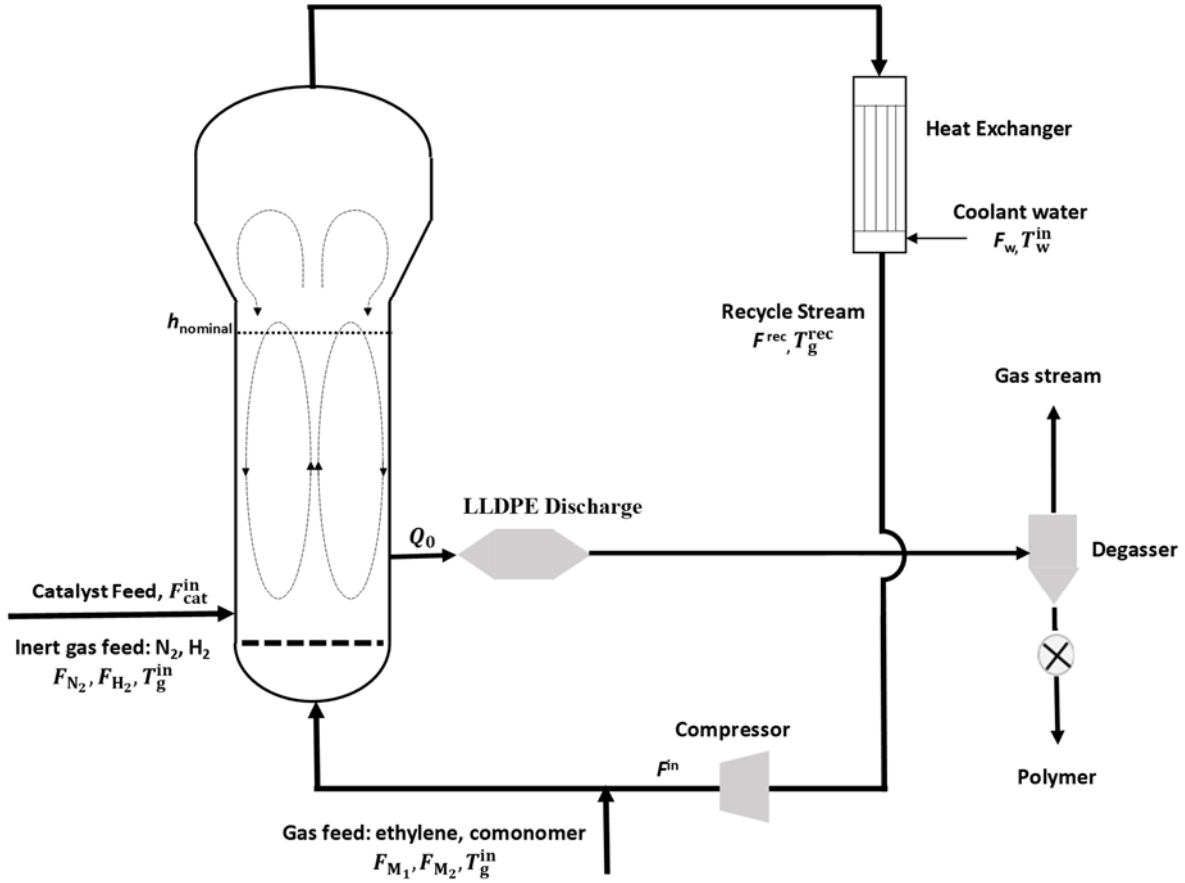

Figure 5. Schematic representation of the polymerization FBR

Approximating the bed by a CSTR, the mass balances of the components present are given in Table S1 and the reaction rates in Table S2 (Supporting Information). It is based on a classical kinetic model of one catalyst site of a Ziegler-Natta type catalyst.[6] The values of the kinetic parameters were taken from Kardous et al. (Table S5).[5] The gas and particles are assumed to have the same temperature (T), uniformly in throughout the bed. Due to the exothermic nature of ethylene polymerization, the temperature of the injected gases (fresh gas and the recycled

gas) is controlled to keep the bed at the desired temperature. Therefore, the recycling stream is equipped with an exchanger to cool the recycled gas. A heat balance of the bed and the exchanger, considered as a series of four small counter flow heat exchangers, was proposed by Chatzidoukas et al.[6], and was used in this work (see Table S3).

2.4 Polymer properties

The correlations used in this work to evaluate the polymer melt index and density are given in Table S4. The polymer density is determined by the percentage of incorporated comonomer, C_{x}. The instantaneous polymer density is then integrated to compute the cumulative density. The melt index is related to the polymer molecular weight, which can be controlled mainly by manipulating the hydrogen flow rate. Both the instantaneous and cumulative polymer molecular weights are calculated and used in the correlation to calculate the instantaneous and cumulative *MI*.

Dynamic off-line optimization and temperature control

In order to ensure fast and safe transitions between different polymer grades, an off line optimization is employed as follows:[7]

$$\min_{\boldsymbol{u}(t)} J(\boldsymbol{u}(t), \boldsymbol{x}(t)),\ t \in [t_0, t_f] \qquad 0.1\ \boldsymbol{u_0} \leq \boldsymbol{u}(t) \leq 5\ \boldsymbol{u_0} \tag{8}$$

where J is the objective function, $\boldsymbol{x}(t)$ the vector of state variables and the manipulated variables of the optimization are the flow rates of hydrogen and comonomer, $\boldsymbol{u}(t) = [F_{\mathrm{H_2}}, F_{\mathrm{com}}]$. Inequality constraints are imposed to define the available ranges of manipulated variables based on the optimal input of the previous grade, $\boldsymbol{u_0}$.

This objective function enables the control of the polymer quality, melt index and density, by considering both the instantaneous and the cumulative properties, with indices c and i respectively, as follows:

$$J(\boldsymbol{u}) = \int_{t_0}^{t_f} w_1 \frac{|MI_i - MI_{sp}|}{MI_{sp}} + w_2 \frac{|MI_c - MI_{sp}|}{MI_{sp}} + w_3 \frac{|\rho_i - \rho_{sp}|}{\rho_{sp}} + w_4 \frac{|\rho_c - \rho_{sp}|}{\rho_{sp}} dt \qquad (9)$$

where w_i (with $i = 1 - 4$) are tuning weights.

In order to ensure the reactor temperature to remain lower than the *MIT* with a safety margin of 5°C, the following algorithm is employed:

- From the desired polymer density, the MIT_0 is predicted using the correlation presented in Figure 2 ($MIT_0 = 0.707\ \rho_p - 556.63$).
- The optimization is run to have the optimal pressure of comonomer required to get the desired polymer density. This pressure is added to the ICA pressure if present, and the fraction of penetrants in the polymer particles is calculated (using the simplified thermodynamic correlation in section 2.2). Then, using Flory-Huggins theory, the *MIT* is calculated. We may face three cases:
  1. If $MIT - 5 > 90$°C, the set-point of the bed temperature, T^{SP}, is kept at its nominal value ($T^{SP} = 90$°C) and there is no risk of sticking.
  2. If $MIT - 5 < 80$°C, this option is not realizable. So, one needs either to reduce the temperature more, or try to use less ICA if present, to produce the desired polymer density without a risk of sticking.
  3. If $80 < MIT < 90$°C, we set $T^{SP} = MIT - 5$. We therefore impose a constraint on *T*. The scenarios shown in this paper are within this case.

Note that all these calculations are inserted within the optimization loop, as the different variables are correlated (temperature, reaction rate, density, etc.).

To control the bed temperature, two PI controllers were employed by manipulating the coolant water temperature entering the exchanger, $T_{\mathrm{w}}^{\mathrm{in}}$, as well as the fresh gas temperature ($T_{\mathrm{g}}^{\mathrm{in}}$).[6] Both control variables allow keeping the bed temperature at the desired value.

$$\begin{bmatrix} T_{\mathrm{w}}^{\mathrm{in}} \\ T_{\mathrm{g}}^{\mathrm{in}} \end{bmatrix} = \begin{bmatrix} k_{\mathrm{p1}} \\ k_{\mathrm{p2}} \end{bmatrix} (T^{\mathrm{SP}} - T) + \begin{bmatrix} k_{\mathrm{i1}} \\ k_{\mathrm{i2}} \end{bmatrix} \int_0^t (T^{\mathrm{SP}} - T)\mathrm{d}t \qquad (10)$$

Where $k_{\mathrm{p}i}$ and $k_{\mathrm{i}i}$ are the proportional and integral tuning parameters.

Simulation results and discussion

Simulations are done using the bed characteristics given in Table S5. The pressure of ethylene (and of ICA if present) is maintained constant during the transition, whereas the comonomer and hydrogen pressures are varied following the optimization results of the flow rates. The bed temperature is kept at its nominal value of 90°C except when there is a risk of sticking where it is decreased, using the PI controllers. The optimization is solved using the function fmincon of Matlab® on a personal computer. In the following sections, arbitrary specifications of grade transitions are implemented from higher to lower polymer density, where the risk of sticking is the highest.

Copolymerization of ethylene with 1-butene

The weighting factors required by the optimization were tuned based on few simulations. The objective was to ensure a rapid convergence of the cumulative properties to the desired set-points (SP), while keeping the instantaneous properties within an acceptable range. The tuning was done with a constant bed temperature, as the weights in the criterion are not affected by the control of *T*. One of the weights was fixed at 1 (here $w_2 = 1$), and the others were varied, as only their ratios has a signification in the criterion. It is important to keep in mind that when modifying the comonomer flow rate to control the density, this also influences the melt index.

However, when modifying the hydrogen flow rate, the density is not influenced. Therefore, it is helpful to give higher weights to the density terms than the melt index, especially when using local optimization methods. This ensures the convergences of both properties. In Figure 6, the weights attributed to the instantaneous and cumulative density are $w_3 = w_4 = 3$. Then, two simulations are compared by varying the weight of the instantaneous melt index, $w_1 = 1.1$ and $w_1 = 0.5$. It can be seen that when higher weights are attributed to cumulative property, it converges faster but this causes important overshoots in the instantaneous property. Indeed, the optimization leads to high variations in the flow rate and pressure of hydrogen. The allowable extent of overshoots should be indicated in the process and properties specifications. In the following, the used values are: $w_1 = 0.5$, $w_2 = 1$, $w_3 = 3$ and $w_4 = 3$. The same values were used for both systems. It is to be noted however that when varying importantly the operating conditions, some adjustment of these factors may be required.

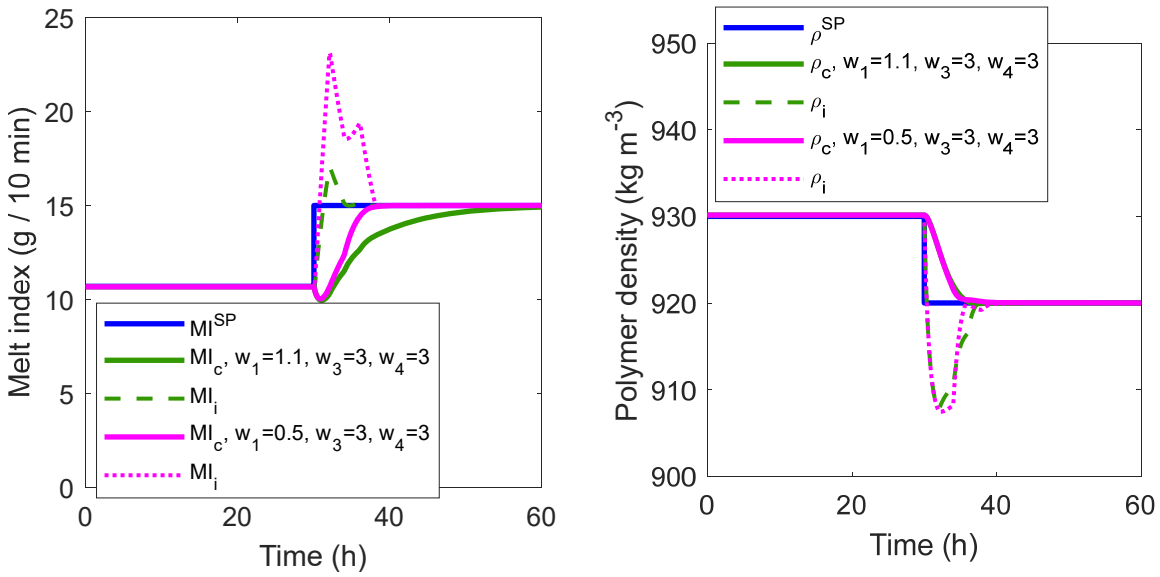

Figure 6. Tuning of w_i during grade transition in ethylene-1-butene copolymerization, without a constraint on T.

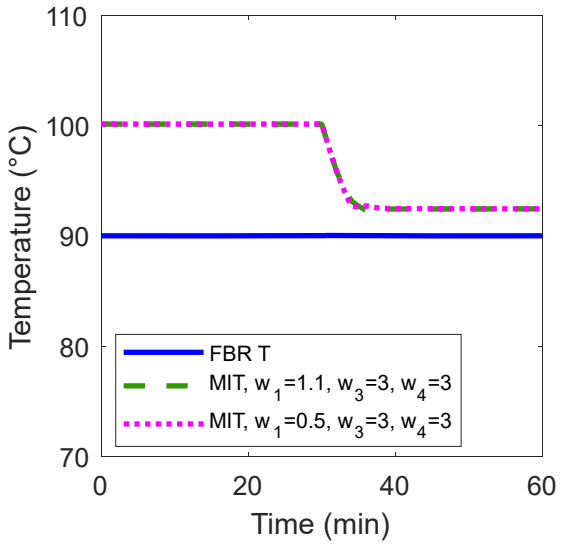

Figure 7. Grade transition in ethylene-1-butene copolymerization, without a constraint on T.

Figure 7 shows the evolution of the particle melting temperature obtained, without constraints on the reactor temperature which was kept at its nominal value 90°C. The *MIT* was predicted by combining the correlation of Hari et al.[22] and the particle swelling by commonomer predicted by the Flory-Huggins theory. During the transition from the first to the second grade, the reduction in the density and the increase in the swelling by comonomer both lead to a decrease of the *MIT*, which gets close to the bed temperature. This might be assumed to be a risky situation as the polymer particles may start sticking and aggregating. Therefore, it is important to consider the time-varying constraint on the bed temperature with the safety margin $T \leq MIT - 5°C$.

The same scenario presented in Figure 6 and Figure 7 was simulated while adding a temperature constraint with a safety margin $T \leq MIT - 5°C$ (Figure 8). It can be seen that the reactor temperature starts cooling during the transition and reaches about 86.7°C for the new grade. By this way, the bed temperature is always about 5°C lower than the onset melting temperature. Note also that the time scale for the convergence of density remains more or less the same, with the temperature being constant or reduced, thanks to the optimization of the comonomer flow

rate. Cooling the bed certainly impacts the reaction rates, but this is necessary to prevent polymer sticking and agglomeration.

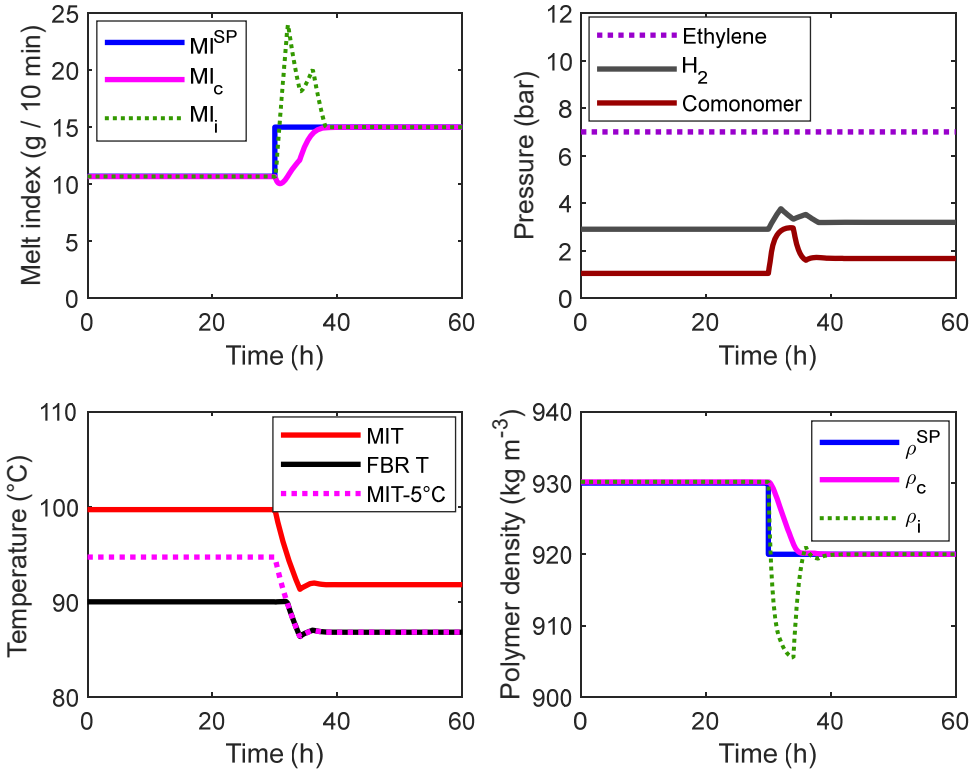

Figure 8. Grade transition in ethylene-1-butene copolymerization under the constraint $T \leq MIT - 5°C$.

Copolymerization of ethylene with 1-hexene

The proposed methodology was evaluated in the second system: ethylene and 1-hexene copolymerization, first without ICA. Note that not only the comonomer is changed but also the operating conditions: with a much lower amount of comonomer (on the range of 0-1 bar) and ethylene pressure around 10 bar. The choice of set-points was also varied.

Figure 9 shows the results of a transition where reducing the polymer density and increasing the melt index are required. The optimization constraint was considered as in the first system, $T \leq MIT - 5°C$. It can be seen that with the polymer density and penetrant concentration of the first grade, the *MIT* was about 96.5°C. Then, during the transition, an injection of

comonomer and hydrogen was realized to increase MI_i and decrease ρ_i. As a result, for the new grade the *MIT* decreased to about 89.4°C as a lower density is produced and more comonomer swells the particles. To avoid particle sticking, the reactor temperature was cooled to 84.4°C. Again, a net decrease in the reaction rate is expected when cooling the bed from 90 to 84.4°C. But, with the closed loop optimization, an adjustment of the properties could be maintained and the sticking constraint was respected. The main observed effect is the slower convergence of the cumulative properties, as less polymer is produced to renew the bed.

It can be noticed that only a small amount of 1-hexene (0-1 bar) can lead to an important decrease of the density of LLDPE and eventual polymer stickiness (compared to the system of 1-butene, with comonomer pressure close to 2 bars for the same density range). This is due to the fact that 1-hexene is more soluble in PE at a given temperature and pressure which leads to a higher reaction rate of the comonomer and so to a lower density. Both the increase in the fraction of penetrant in the particles and the decrease in density lead to a faster decrease in the *MIT*.

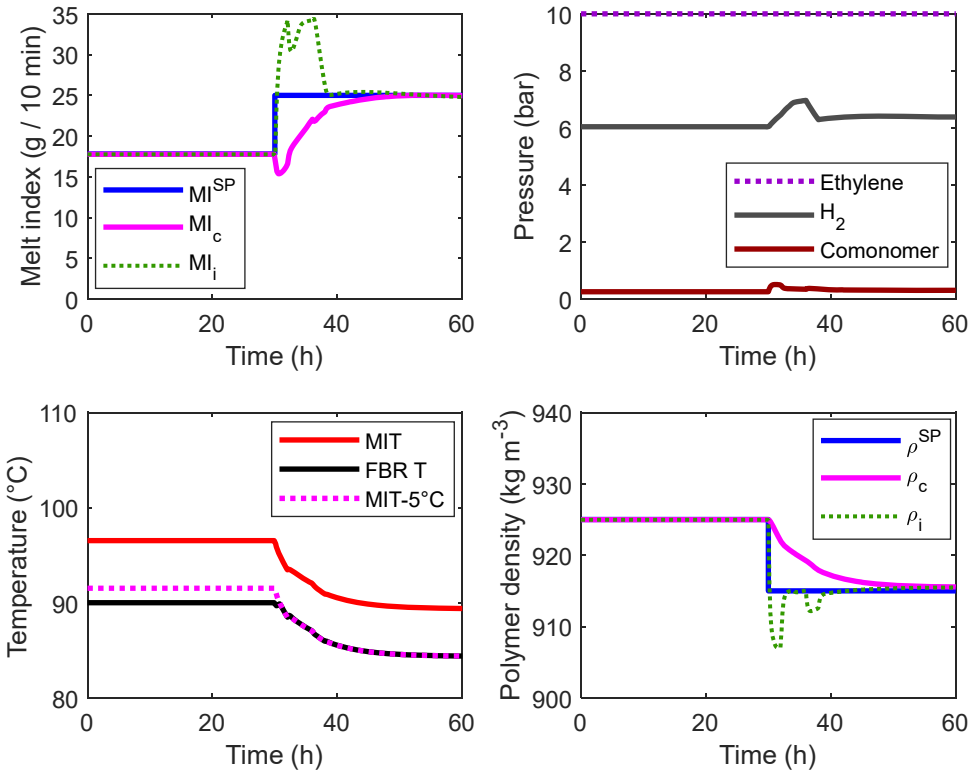

Figure 9. Grade transition in ethylene-1-hexene copolymerization under constraint $T \leq MIT - 5°C$.

Copolymerization of ethylene with 1-hexene in presence of n-hexane

In this section, the second system ethylene and 1-hexene copolymerization is considered in presence of ICA n-hexane. Figure 10 shows the optimization results of this system, with constraint on the bed temperature. The ICA pressure was 1.2 bar. Adding an ICA to the system affects polymer swelling by ethylene and penetrants. This leads to an increase in the reaction rates of monomer and comonomer, which affects the polymer properties. Moreover, due to the higher swelling of the particle with penetrants, the *MIT* decreases and the risk of sticking increases. In this simulation, it was necessary to reduce the bed temperature to 82°C to avoid sticking. Note that the set-point of polymer density in the new grade is 920 kg m^{-3} in this scenario while it was 915 kg m^{-3} in the scenario without ICA (with a similar transition of *MI*).

In the presence of this amount of ICA, it is not possible to produce a polymer of low density 915 kg m^{-3} at temperature higher than 80°C without avoiding sticking.

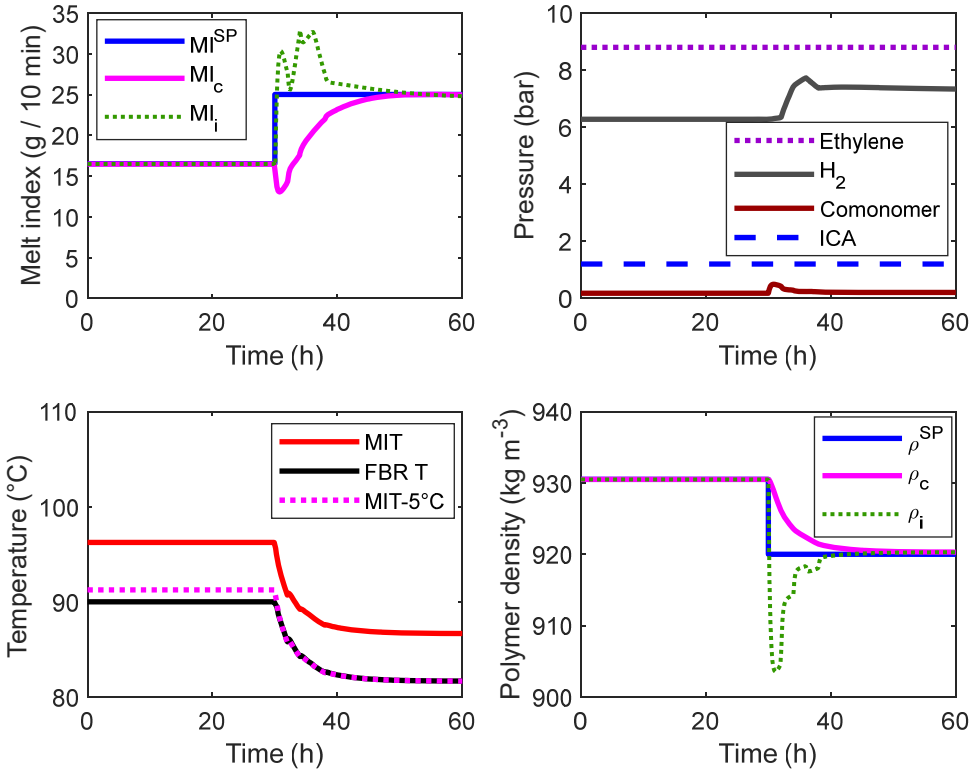

Figure 10. Grade transition in ethylene-1-hexene copolymerization, in presence of n-hexane, under constraint $T \leq MIT - 5°C$.

In Figure 6, it was shown that a good tuning of the parameters w_i allows reducing the overshoots in the instantaneous properties MIi and ρi. Another efficient way of ensuring these instantaneous properties to remain within a specific range is to consider inequality constraints on the outputs during the optimization. Figure 11 shows a scenario of optimization with constraints on the instantaneous properties. Compared to Figure 10, it can be seen that the overshoots were decreases and remained within the allowed margin. However, this slowed down the convergence of the cumulative properties. Also, considering constraints in the optimization increases the computation time. However, in this manner, one may ensure a good control of the instantaneous properties. Indeed, such overshoots lead to wider distributions of

the properties (e.g. polymer molecular weight or branches), which are difficult to model and for which the effects on the properties such as the *MIT* are not well-known.

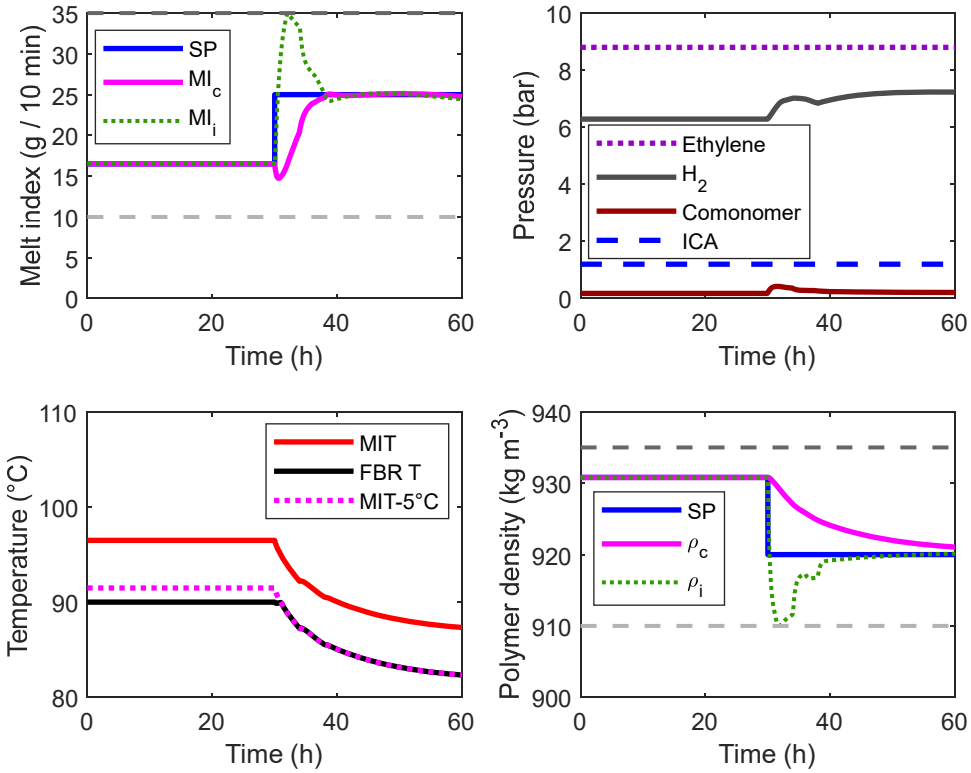

Figure 11. Grade transition in ethylene-1-hexene copolymerization, in presence of n-hexane under constraint $T \leq MIT - 5°C$, as well as constraints on the outputs MIi and ρi (gray dotted lines).

Conclusions

This work provides an optimization strategy of FBR polymerization process during grade transition that allows controlling the end-use properties of polymer grades (polymer melt index and density) while avoiding particle stickiness and agglomeration. A model based on data collected from the patent literature combined to Flory-Huggins theory was used to predict the onset melting temperature of particles in the presence of penetrants. A control of the bed temperature is done in a way to respect the constraint of the *MIT*. The *MIT* is considered to be the most representative of the sticking temperature.

The effect of comonomer on the particle sticking temperature was evaluated by two ways: first it leads to the creation of more branches in the polymer chain and so to a decrease in the polymer density and crystallinity; second it may plasticize the particle and act as sticking promoter when dissolved in the particle; both effects lead to a decrease in the *MIT*. Similarly, the presence of ICA leads to a greater swelling by the penetrants which leads to a decrease in the *MIT* and increases the risk of sticking.

The employment of adapted thermodynamic models is also highlighted, since in a ternary system the gases may influence the solubility of each other, which affects the reaction rates of monomer and comonomer, and therefore of the properties (polymer melt index, density and particle softening temperature).

Supporting Information

This information is available free of charge via the Internet at http://pubs.acs.org/.

Acknowledgements

This work was financed by the Agence Nationale de la Recherche, under Thermopoly project grant N° ANR-16-CE93-0001-01.

Table of Contents graphic

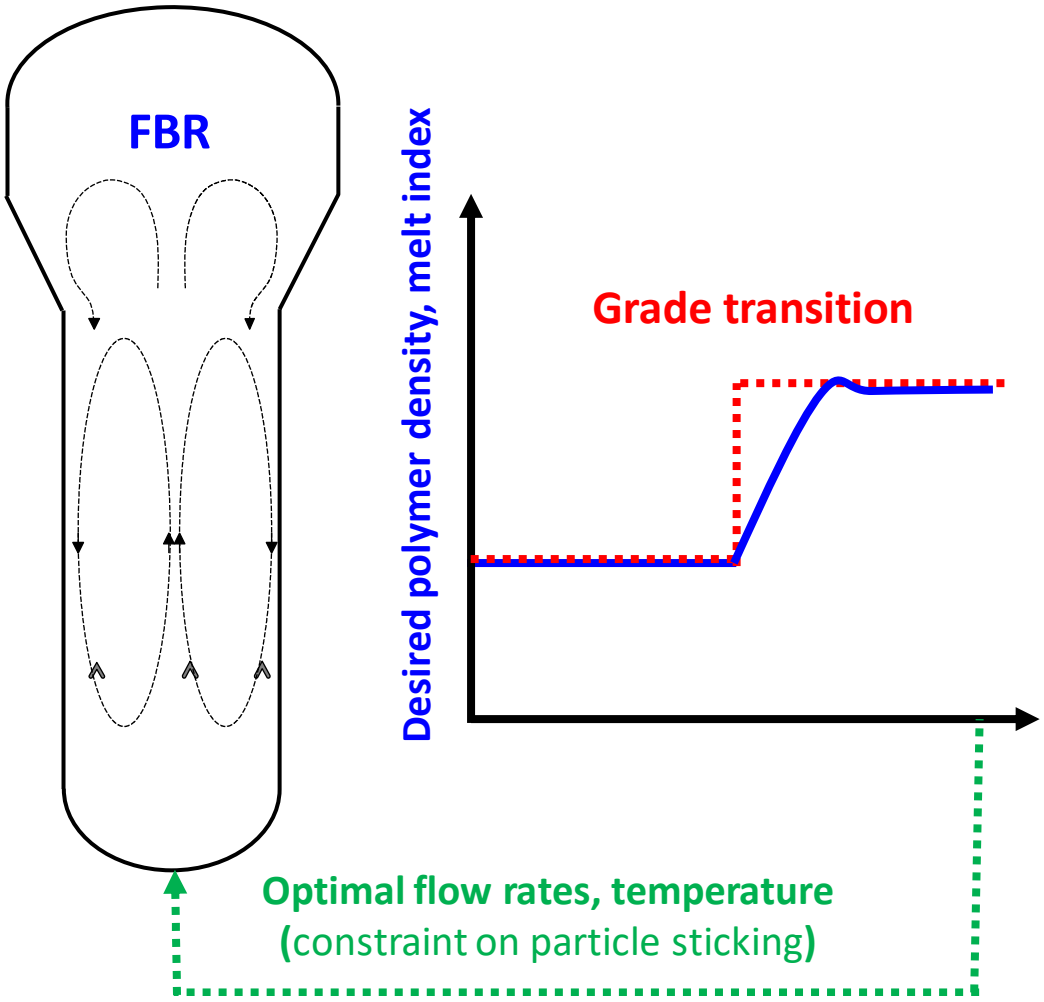

References

(1) McKenna, T. F. L. Condensed Mode Cooling of Ethylene Polymerization in Fluidized Bed Reactors. *Macromolecular Reaction Engineering* **2019**, *13* (2), 1800026. https://doi.org/10.1002/mren.201800026.

(2) Banaszak, B. J.; Lo, D.; Widya, T.; Ray, W. H.; de Pablo, J. J.; Novak, A.; Kosek, J. Ethylene and 1-Hexene Sorption in LLDPE under Typical Gas Phase Reactor Conditions: A Priori Simulation and Modeling for Prediction of Experimental Observations. *Macromolecules* **2004**, *37* (24), 9139–9150. https://doi.org/10.1021/ma0491107.

(3) Bashir, M. A.; Ali, M. A.; Kanellopoulos, V.; Seppälä, J.; Kokko, E.; Vijay, S. The Effect of Pure Component Characteristic Parameters on Sanchez–Lacombe Equation-of-State Predictive Capabilities. *Macromolecular Reaction Engineering* **2013**, *7* (5), 193–204. https://doi.org/10.1002/mren.201200054.

(4) Alizadeh, A. Study of Sorption, Heat and Mass Transfer during Condensed Mode Operation of Gas Phase Ethylene Polymerization on Supported Catalyst, Queen's University, Kingston, Ontario, Canada, 2014.

(5) Kardous, S.; McKenna, T. F. L.; Sheibat-Othman, N. Thermodynamic Effects on Grade Transition of Polyethylene Polymerization in Fluidized Bed Reactors. *Macromolecular Reaction Engineering n/a* (n/a), 2000013. https://doi.org/10.1002/mren.202000013.

(6) Chatzidoukas, C.; Perkins, J. D.; Pistikopoulos, E. N.; Kiparissides, C. Optimal Grade Transition and Selection of Closed-Loop Controllers in a Gas-Phase Olefin Polymerization Fluidized Bed Reactor. *Chemical Engineering Science* **2003**, *58* (16), 3643–3658. https://doi.org/10.1016/S0009-2509(03)00223-9.

(7) McAuley, K. B.; MacGregor, J. F. Optimal Grade Transitions in a Gas Phase Polyethylene Reactor. *AIChE J.* **1992**, *38* (10), 1564–1576. https://doi.org/10.1002/aic.690381008.

(8) McAuley, K. B.; MacGregor, J. F.; Hamielec, A. E. A Kinetic Model for Industrial Gas-Phase Ethylene Copolymerization. *AIChE Journal* **1990**, *36* (6), 837–850. https://doi.org/10.1002/aic.690360605.

(9) Soares, J. B. P.; McKenna, T. F. L. Polyolefin Reaction Engineering. 345.

(10) Dadebo, S. A.; McAuley, K. B.; McLellan, P. J. INTERACTIONS BETWEEN PRODUCTION RATE OPTIMIZATION AND TEMPERATURE CONTROL IN GAS PHASE POLYETHYLENE REACTORS. In *Dynamics and Control of Chemical Reactors, Distillation Columns and Batch Processes (Dycord'95)*; Rawlings, J. B., Ed.; IFAC Postprint Volume; Pergamon: Oxford, 1995; pp 293–298. https://doi.org/10.1016/B978-0-08-042368-5.50050-2.

(11) Ghasem, N. M.; Ang, W. L.; Hussain, M. A. Dynamics and Stability of Ethylene Polymerization in Multizone Circulating Reactors. *Korean J. Chem. Eng.* **2009**, *26* (3), 603–611. https://doi.org/10.1007/s11814-009-0102-1.

(12) Chatzidoukas, C. Control and Dynamic Optimisation of Polymerization Reaction Processes, University of London, London, 2004.

(13) Dadebo, S. A.; Bell, M. L.; McLellan, P. J.; McAuley, K. B. Temperature Control of Industrial Gas Phase Polyethylene Reactors. *Journal of Process Control* **1997**, *7* (2), 83–95. https://doi.org/10.1016/S0959-1524(96)00016-9.

(14) Rahimpour, M. R.; Fathikalajahi, J.; Moghtaderi, B.; Farahani, A. N. A Grade Transition Strategy for the Prevention of Melting and Agglomeration of Particles in an Ethylene Polymerization Reactor. *Chem. Eng. Technol.* **2005**, *28* (7), 831–841. https://doi.org/10.1002/ceat.200500055.

(15) Turkistani, N. M. Fluidized Bed Methods for Making Polymers. US6759489B1, July 6, 2004.
(16) Chmelar, J.; Matuska, P.; Gregor, T.; Bobak, M.; Fantinel, F.; Kosek, J. Softening of Polyethylene Powders at Reactor Conditions. *Chemical Engineering Journal* **2013**, *228*, 907–916. https://doi.org/10.1016/j.cej.2013.05.069.
(17) DeChellis, M. L.; Griffin, J. R.; Muhle, M. E. Process for Polymerizing Monomers in Fluidized Beds. US5405922A, April 11, 1995.
(18) Hagerty, R. O.; Stavens, K. B.; DeChellis, M. L.; Fischbuch, D. B.; Farley, J. M. Polymerization Process. US7122607B2, October 17, 2006.
(19) Singh, D.; Hinds, S.; Fischbuch, B.; Vey, N. A. Gas-Phase Process. US20050182207A1, August 18, 2005.
(20) Hendrickson, G. G. Method for Operating a Gas Phase Polymerization Reactor. US7531606B2, May 12, 2009.
(21) *Exxon Mobile Product Data Sheets, Https://Www.Exxonmobilchemical.Com/En/Products/Polyethylene, Product Data Sheets, Accessed 12 October 2020.*; 2020.
(22) Hari, A. S.; Savatzky, B. J.; Glowczwski, D. M.; Cao, X. Controlling a Polyolefin Reaction. US 9,718,896 B2, 2015.
(23) Goode, M. G.; Blood, M. W.; Sheard, W. G. High Condensing Mode Polyolefin Production under Turbulent Conditions in a Fluidized Bed. US6391985B1, May 21, 2002.
(24) Schneider, M. J.; Mülhaupt, R. Influence of Indenyl Ligand Substitution Pattern on Metallocene-Catalyzed Propene Copolymerization with 1-Octene. *Macromolecular Chemistry and Physics* **1997**, *198* (4), 1121–1129. https://doi.org/10.1002/macp.1997.021980415.
(25) Kamal, M. R.; Feng, L.; Huang, T. A Generalized Equation for the Prediction of Melting Temperatures of Homopolymers and Copolymers. *Can. J. Chem. Eng.* **2002**, *80* (3), 432–442. https://doi.org/10.1002/cjce.5450800312.
(26) Flory, P. J. Thermodynamics of Crystallization in High Polymers. IV. A Theory of Crystalline States and Fusion in Polymers, Copolymers, and Their Mixtures with Diluents. *The Journal of Chemical Physics* **1949**, *17* (3), 223–240. https://doi.org/10.1063/1.1747230.
(27) Asano, T.; Noble, W. J. L. "Void" and "Expansion" Volume Contributions to Reaction and Activation Volumes of Nearly Nonpolar Reactions. *The Review of Physical Chemistry of Japan* **1974**, *43* (2), 82–91.
(28) Fried, Joel. R. *Polymer Science and Technology*, Pertinance Hall.; Saddle River, 1995.
(29) JR, D. N. T.; Markel, E. J. Polymerization Reaction Monitoring with Determination of Induced Condensing Agent Concentration for Preventing Discontinuity Events. US7754830B2, July 13, 2010.
(30) G. Mikos, A.; A. Peppas, N. Flory Interaction Parameter χ for Hydrophilic Copolymers with Water. *Biomaterials* **1988**, *9* (5), 419–423. https://doi.org/10.1016/0142-9612(88)90006-3.
(31) Titow, W. V. *PVC Technology*, Fourth.; Elsevier Applied Science Publishers Ltd: London and New York, 1984.
(32) Marsac, P. J.; Li, T.; Taylor, L. S. Estimation of Drug–Polymer Miscibility and Solubility in Amorphous Solid Dispersions Using Experimentally Determined Interaction Parameters. *Pharm Res* **2008**, *26* (1), 139. https://doi.org/10.1007/s11095-008-9721-1.
(33) Muhle, M. E.; Pannell, R. B.; Markel, E. J.; Hagerty, robert O. Systems and Methods for Monitoring a Polymerization Reaction. US 8,383,739 B2, 2013.

(34) de Camargo Forte, M. M.; da Cunha, F. O. V.; dos Santos, J. H. Z.; Zacca, J. J. Ethylene and 1-Butene Copolymerization Catalyzed by a Ziegler–Natta/Metallocene Hybrid Catalyst through a 23 Factorial Experimental Design. *Polymer* **2003**, *44* (5), 1377–1384. https://doi.org/10.1016/S0032-3861(02)00874-1.

(35) Alves, R.; Bashir, M. A.; McKenna, T. F. L. Modeling Condensed Mode Cooling for Ethylene Polymerization: Part II. Impact of Induced Condensing Agents on Ethylene Polymerization in an FBR Operating in Super-Dry Mode. *Ind. Eng. Chem. Res.* **2017**, *56* (46), 13582–13593. https://doi.org/10.1021/acs.iecr.7b02963.

(36) Sun, J.; Wang, H.; Chen, M.; Ye, J.; Jiang, B.; Wang, J.; Yang, Y.; Ren, C. Solubility Measurement of Hydrogen, Ethylene, and 1-Hexene in Polyethylene Films through an Intelligent Gravimetric Analyzer. *Journal of Applied Polymer Science* **2017**, *134* (8). https://doi.org/10.1002/app.44507.

(37) Ben Mrad, A.; Sheibat-Othman, N.; Hill, J.; Bartke, M.; McKenna, T. F. L. A Novel Approach for the Estimation of the Sanchez-Lacombe Interaction Parameters for the Solubility of Ternary Polyolefins Systems. *Chemical Engineering Journal* **2020**, 127778. https://doi.org/10.1016/j.cej.2020.127778.

(38) Touloupides, V.; Kanellopoulos, V.; Pladis, P.; Kiparissides, C.; Mignon, D.; Van-Grambezen, P. Modeling and Simulation of an Industrial Slurry-Phase Catalytic Olefin Polymerization Reactor Series. *Chemical Engineering Science* **2010**, *65* (10), 3208–3222. https://doi.org/10.1016/j.ces.2010.02.014.

(39) Kanellopoulos, V.; Mouratides, D.; Pladis, P.; Kiparissides, C. Prediction of Solubility of α-Olefins in Polyolefins Using a Combined Equation of StateMolecular Dynamics Approach. *Ind. Eng. Chem. Res.* **2006**, *45* (17), 5870–5878. https://doi.org/10.1021/ie060137j.

(40) Moore, S. J.; Wanke, S. E. Solubility of Ethylene, 1-Butene and 1-Hexene in Polyethylenes. *Chemical Engineering Science* **2001**, *56* (13), 4121–4129. https://doi.org/10.1016/S0009-2509(01)00082-3.

(41) Yao, W.; Hu, X.; Yang, Y. Modeling the Solubility of Ternary Mixtures of Ethylene, Iso-Pentane, n-Hexane in Semicrystalline Polyethylene. *Journal of Applied Polymer Science* **2007**, *104* (6), 3654–3662. https://doi.org/10.1002/app.26137.

(42) Mann, J. Transport Processes and Unit Operations. *The Chemical Engineering Journal* **1980**, *20* (1), 82. https://doi.org/10.1016/0300-9467(80)85013-1.

(43) Kunii, D.; Levenspiel, O. Bubbling Bed Model. Model for Flow of Gas through a Fluidized Bed. *Ind. Eng. Chem. Fund.* **1968**, *7* (3), 446–452. https://doi.org/10.1021/i160027a016.